Uptake of dissolved inorganic and organic nitrogen by the benthic toxic dinoflagellate Ostreopsis cf. ovata

Cécile Jauzein, Douglas Couet, Thierry Blasco, Rodolphe Lemée

Uptake of dissolved inorganic and organic nitrogen by the benthic toxic dinoflagellate *Ostreopsis* cf. *ovata*

Cécile Jauzein[a,b,*], Douglas Couet[a], Thierry Blasco[a], Rodolphe Lemée[a]

[a] Sorbonne Universités, UPMC Univ Paris 06, INSU-CNRS, Laboratoire d'Océanographie de Villefranche, Villefranche sur mer, France

[b] IFREMER, Centre de Brest, DYNECO PELAGOS, F-29280 Plouzané, France

*Corresponding author

E-mail: cecile.jauzein@ifremer.fr

Abbreviations: Elemental Analysis – Isotope Ratio Mass Spectrometry (EA-IRMS), particulate carbon (PC), particulate nitrogen (PN)

Abstract:

Environmental factors that shape dynamics of benthic toxic blooms are largely unknown. In particular, for the toxic dinoflagellate *Ostreopsis* cf. *ovata*, the importance of the availability of nutrients and the contribution of the inorganic and organic pools to growth need to be quantified in marine coastal environments. The present study aimed at characterizing N-uptake of dissolved inorganic and organic sources by *O*. cf. *ovata* cells, using the ^{15}N-labelling technique. Experiments were conducted taking into account potential interactions between nutrient uptake systems as well as variations with the diel cycle. Uptake abilities of *O.* cf. *ovata* were parameterized for ammonium (NH_4^+), nitrate (NO_3^-) and N-urea, from the estimation of kinetic and inhibition parameters. In the range of 0 to 10 µmol N L^{-1}, kinetic curves showed a clear preference pattern following the ranking $NH_4^+ > NO_3^- >$ N-urea, where the preferential uptake of NH_4^+ relative to NO_3^- was accentuated by an inhibitory effect of NH_4^+ concentration on NO_3^- uptake capabilities. Conversely, under high nutrient concentrations, the preference for NH_4^+ relative to NO_3^- was largely reduced, probably because of the existence of a low-affinity high capacity inducible NO_3^- uptake system. Ability to take up nutrients in darkness could not be defined as a competitive advantage for *O*. cf. *ovata*. Species competitiveness can also be defined from nutrient uptake kinetic parameters. A strong affinity for NH_4^+ was observed for *O.* cf. *ovata* cells that may partly explain the success of this toxic species during the summer season in the Bay of Villefranche-sur-mer (France).

Keywords: Uptake; nitrogen; dinoflagellate; *Ostreopsis*; kinetics; interactions

1. Introduction

Benthic harmful algal blooms represent an increasing threat to human and environmental health worldwide (Parsons et al., 2012; Rhodes, 2011). Toxic dinoflagellates belonging to the genus *Ostreopsis* Schmidt are common components of tropical epibenthic microalgae communities and have also been reported in several temperate waters, including coastal waters of the Mediterranean Sea (Vila et al., 2001), New Zealand (Rhodes et al., 2000) or Japan (Taniyama et al., 2003). Along the Mediterranean coasts, massive *Ostreopsis* cf. *ovata* blooms regularly occurred during the summer season and early fall (e.g. Aligizaki and Nikolaidis, 2006; Mangialajo et al., 2011). Some of them were associated with serious cases of human health disorders (Brescianini et al., 2006; Vila et al., 2016). Symptoms of human illnesses include skin irritations, fever or broncho-constriction, partly due to exposure to toxic marine aerosols (Ciminiello et al., 2014). Blooms of *O*. cf *ovata* can also have deleterious effects on benthic marine invertebrates (Accoroni et al., 2011; Guidi-Guilvard et al., 2012; Pagliara and Caroppo, 2012; Gorbi et al., 2013). The toxicity of *O*. cf *ovata* is associated with the presence of palytoxin-like compounds that include putative palytoxin and ovatoxins-a, b, c, d, e and f (Uchida et al., 2013; Brissard et al., 2014), and mascarenotoxins-a and c (Rossi et al., 2010; Scalco et al., 2012). Palytoxin-like compounds have already been found in Mediterranean fauna (Biré et al. 2015) but no related food poisoning has been reported.

The processes that shape dynamics of benthic dinoflagellate populations and facilitate the development of specific toxic species are still poorly understood, mainly because benthic dinoflagellates have received considerably less attention than their planktonic counterparts (Parsons et al. 2012). Among potential controlling factors, temperature may represent a key factor in the seasonality of *O*. cf *ovata* blooms in temperate areas (Mangialajo et al., 2008; Accoroni et al., 2014; Accoroni and Totti, 2016). The control of bloom dynamics by water temperate has still to be clarified, however, as its appeared to vary with geographical areas

(Accoroni and Totti, 2016). Concerning other physical parameters, several studies reported higher abundances of *O*. cf *ovata* in sheltered sites compared to the ones exposed to wave action (e.g. Totti et al., 2010; Selina et al., 2014). This suggests that hydrodynamic conditions can have strong effects on bloom development and maintenance; according to Accoroni and Totti (2016), this influence of hydrodynamics on *O*. cf *ovata* bloom may be particularly pronounced under high levels of abundance (Accoroni and Totti, 2016).

The growth and maintenance of microalgae populations are also directly dependent on nutritive sources that are fueling the blooms. The regulation of *O.* cf. *ovata* bloom dynamics by the nutrient resource is largely unknown. Cells of *Ostreopsis* are expected to be mixotrophic, able to complete their autotrophic growth (based on photosynthesis and uptake of inorganic sources) by the use of organic matter (Burkholder et al., 2008). Among potential organic sources, the phagotrophy of preys by *Ostreopsis* cells was investigated (Faust et al., 1996; Barone, 2007) but is still a matter of debate (Escalera et al., 2014). The potential use of dissolved organic phosphorus by *O*. cf *ovata* cells was tested by Pistocchi et al. (2014), when the uptake of dissolved organic nitrogen sources has not been analyzed yet. Concerning the inorganic sources of nutrients, previous studies reported conflicting results regarding relationships between nutrient availability and occurrence of *Ostreopsis* blooms (Accoroni and Totti, 2016). Several field studies conducted in the NW Mediterranean Sea did not show any relationship between epiphytic *O.* cf. *ovata* abundances and concentrations of dissolved inorganic nutrients (dissolved inorganic nitrogen, DIN, and phosphate) (Vila et al., 2001; Accoroni et al., 2011). Conversely, Parsons and Preskitt (2007) found that *Ostreopsis* sp.1 abundance was positively correlated with nutrient concentrations in the waters surrounding Hawai'i. A positive correlation between phosphate concentration and *O*. cf. *ovata* abundance was also reported by Cohu et al. (2013) in the NW Mediterranean Sea. In the Northern Adriatic Sea, phosphate pulses

in the bloom onset period may possibly stimulate *O* cf. *ovata* growth in these coastal waters (Accoroni et al., 2015).

The importance of the availability of nutrient sources and their contribution to *O* cf. *ovata* growth during bloom development and maintenance need to be quantified in marine coastal environments. In the present study, the control of *O* cf. *ovata* growth by several nitrogen (N) sources was investigated under controlled conditions, using cultures. The main goal of the present work was to characterize N-uptake of dissolved inorganic and organic sources, using the ^{15}N-labelling technique and taking into account potential interactions between nutrient uptake systems as well as variations with the diel cycle.

2. Material and methods

2.1. Culture conditions

Two strains of *Ostreopsis* cf. *ovata*, MCCV 054 and MCCV 055, were obtained from the Mediterranean Culture Collection of Villefranche (MCCV). They were both isolated in 2014 from Villefranche Bay, South of France (43°41′34.83″ N and 7°18′31.66″ E), during the same bloom event. Non-axenic stock cultures were grown in modified K/10 medium (originally defined by Keller et al. (1987)), where addition of silicate and Tris base was omitted, phosphorus was added as KH_2PO_4 (final concentration of 4 µM) and ZnSO4 was added at a final concentration of 0.08 nM. Culture medium was prepared using autoclaved old seawater filtered on 0.2 µm (FSW) at salinity 38. Cultures were maintained at 23°C, under 250 µmol photons m^{-2} s^{-1}, with a 16:8 h light:dark cycle. Stock cultures were grown in batch mode without bubbling, in 15 mL of culture medium. Culture flasks were maintained in flat culturing conditions in order to optimize the surface area for gas exchange and growth of benthic cells. Before each experiment, one stock culture in exponential phase of growth was successively

diluted in order to scale up the culture volume from 15 ml (in flask of 25 cm² surface area) to 350 ml (in flask of 300 cm² surface area). The final large volume culture was used to inoculate three or four replicated cultures of 350 ml. Experiments were run using a set of replicated cultures in exponential phase and characterized by a cell density higher than 1,500 cell ml^{-1}.

2.2. Micro-algal cell resuspension in low N medium

Experiments were conducted under controlled conditions of nitrogen (N) availability in order to help for a precise characterization of N-uptake capabilities of *O.* cf. *ovata* cells. Each experiment started with the resuspension of micro-algal cells in culture medium where no NH_4^+ or NO_3^- addition was performed (–N medium). Concentrations of NH_4^+ and NO_3^- were determined for the –N medium used for running the experiments. Full resuspension of *O.* cf. *ovata* cells was completed in about 1h. Cells were collected on an 8 or 10 µm mesh size net by gravity filtration, then rinsed with –N medium before being resuspended in –N medium. To ensure that the net was not clogged due to mucus accumulation, these collection, rinsing and resuspension steps were performed on successive aliquots of 35 or 40 mL of culture and a new piece of net was used every four aliquots. A gentle agitation of the net in –N medium did not allow for passive resuspension of *O.* cf. *ovata* cells. Thus, for each aliquot of culture, micro-algal cells concentrated on the net were collected by pipetting repeatedly and carefully ~1 ml of –N medium above the net, then this volume was finally poured in a culture flask (75 cm² surface area) filled with 40 mL of –N medium. The resuspension and rinsing steps allowed for the removal of most of the bacteria present in the growth medium and limited their contribution in the resuspended cultures (Raush de Traubenberg and Soyer-Gobillard, 1990).

The resuspended culture flasks were kept aside in the culture chamber, under initial culture conditions, during 1-2h before starting the incubations. This lag reduced the potential

impact of stress associated with the resuspension step on uptake rates and also contributed to start incubations under really low N concentrations.

2.3. Kinetic experiments

Uptake kinetics of three potential N-sources, nitrate (NO_3^-), ammonium (NH_4^+) and urea, were characterized for the two *O.* cf. *ovata* strains, MCCV 054 and MCCV 055. For each strain, *O.* cf. *ovata* cells were resuspended from three replicated cultures of 350 ml in exponential phase. Each mother culture allowed for the creation of one series of eight 40 ml samples and was used to characterize the uptake kinetics of one N-source. Incubations started with the addition of ^{15}N ($^{15}NO_3^-$, $^{15}NH_4^+$ or ^{15}N-urea) at eight graded concentrations (0.1, 0.2, 0.5, 1, 2, 3, 5, and 10 µmol N L^{-1}). Samples were incubated for 1h under initial culture conditions. At the end of the incubation, samples were filtered through precombusted (4 h at 450°C) A/E filters (Gelman Sciences) and rinsed with 20 mL of FSW. Filters were dried at 60°C overnight and analyzed by EA-IRMS (Elemental Analysis – Isotope Ratio Mass Spectrometry) for measurements of particulate carbon (PC), particulate nitrogen (PN) and $^{15}N/^{14}N$ isotopic ratios.

An additional experiment was conducted in order to characterize N-urea uptake capabilities of *O.* cf. *ovata* cells taking into account the potential role of preconditioning effects. Cells of *O.* cf. *ovata* were grown on a modified K/10 medium containing three potential N-sources: NO_3^- added at 28.8 µmol N L^{-1} and NH_4^+ and N-urea added at 5 µmol N L^{-1}. These growth conditions were maintained during several culture transfers in batch mode. Then, one culture of 350 mL in exponential phase was used for running a replicated kinetic experiment, in order to estimate N-urea uptake rates along a concentration gradient of 0 – 10 µmol N L^{-1}.

2.4. Interaction experiments

166 An experiment was run in order to characterize the potential interaction between NH_4^+
167 and NO_3^- uptake. Four replicated cultures of 350 mL (MCCV 054) were used to carry out two
168 successive series of incubations, one testing the influence of NH_4^+ on the maximal uptake rate
169 of NO_3^-, and the other the influence NO_3^- on the maximal uptake rate of NH_4^+. During each part
170 of the experiment, the uptake rate of one nutrient, added at a reference concentration of 10 µmol
171 N L^{-1}, was measured as a function of the increasing concentration of the other nutrient (0, 0.1,
172 0.2, 0.5, 1, 2, 3, 5, and 10 µmol N L^{-1}). For each set, two series of incubations were performed
173 in parallel in order to simultaneously assay uptake rates of both nutrients (NH_4^+ and NO_3^-) for
174 all nutritive conditions. These coupled incubations were based on the same nutrient regime,
175 with only one of the two N-sources labeled with ^{15}N: for one series of samples, the nutrient
176 added under various concentration (0-10 µmol N L^{-1}) was labeled with ^{15}N and, for the other
177 series of samples, the nutrient added at saturating concentration (10 µmol N L^{-1}) was labeled
178 with ^{15}N. Incubations started with the addition of $^{15}NH_4^+$ or $^{15}NO_3^-$ into 40 mL samples and
179 lasted 1h. Incubations ended with the filtration of samples through precombusted (4 h at 450°C)
180 A/E filters (Gelman Sciences). Filters were rinsed with 20 mL of FSW, then dried at 60°C
181 overnight. Analyses were run using EA-IRMS in order to obtain measurements of PN, PC and
182 $^{15}N/^{14}N$ isotopic ratios.
183
184 **2.5. Diel cycle experiments**
185 Variations of NH_4^+- and NO_3^--uptake by *O.* cf. *ovata* cells were investigated over the
186 diel cycle. For each N-source, three replicated cultures of 350 ml (MCCV 054) were used and
187 allowed for the preparation of three series of ten resuspended samples, each of them containing
188 40 mL of –N medium. At the beginning of the incubations, all samples were spiked with a
189 solution of ^{15}N ($^{15}NH_4^+$ or $^{15}NO_3^-$) at 100 µmol N L^{-1} final concentration and were immediately
190 replaced in the culture chamber under initial conditions. This level of concentration was used

191 to ensure N-sufficient conditions all along the experiment duration. Regular stops in the
192 incubations were done during a 24h survey (every 3 h during light periods and three times
193 during the dark phase). At each stop, three samples were taken, one originating from each of
194 the replicated mother cultures. Cells of *O.* cf. *ovata* were collected on precombusted (4 h at
195 450°C) A/E filters (Gelman Sciences) and rinsed with 20 mL of FSW. Half of the samples were
196 used to follow nutrient concentrations during the experiment, collecting 20 mL of the culture
197 filtrate during microalgal cell collection (before the rinsing step). Filters were finally dried at
198 60°C overnight, then analyzed by EA-IRMS in order to obtain measurements of PN, PC and
199 $^{15}N/^{14}N$ isotopic ratios.
200
201 **2.6. Cell counts and nutrient analysis**
202 Growth rate was estimated for each mother culture used for running experiments, from
203 measurements of cell density done just before the resuspension step and 24h earlier. These
204 growth rate estimations allowed to verify that *O.* cf. *ovata* cells were growing under optimal
205 growth conditions when incubations started. For sampling, three 2 mL-aliquots of culture were
206 taken after a gentle mixing of the culture and pooled together before counting. Samples were
207 fixed with acidic lugol solution at 1% (vol/vol) final concentration and stored at +4°C until
208 analysis. Cell counts were done in triplicate using a 1 mL Sedgewick rafter counting chamber.
209 Growth rates were calculated according to Guillard (1973), using the following formula:
210 $$\mu = \frac{\ln(C2) - \ln(C1)}{t2 - t1}$$
211 where μ is the growth rate (d^{-1}), C_1 and C_2 are the cell concentrations at time 1 (t_1, d) and time
212 2 (t_2, d), respectively.
213 Measurements of NH_4^+ concentrations were performed few hours after sampling, using
214 the fluorometric method (Taylor et al., 2007). Samples for estimations of NO_3^- concentration
215 were immediately frozen at -20°C and stored until analysis. Concentrations of NO_3^- were

measured using an automated colourimetry system (Seal Analytical continuous flow AutoAnalyser III, AA3)) as described by Bendschneider and Robienson (1952).

2.7. N-uptake measurements and kinetic parameters

For determination of PN, PC and $^{15}N/^{14}N$ isotopic ratios, EA-IRMS experiments were done with an Elementar Vario Pyro Cube analyzer in CN mode (combustion oven 920°C, reduction oven 600°C) coupled to an Isoprime 100 IRMS (Isotope Resolved Mass Spectrometer). Calibration of measurements was performed with certified caffeine (AIEA-600) and other laboratory standards (commercially available glycine (Sigma), acetinalide (Merck)).

Uptake rates (V in h^{-1}) were calculated from the ^{15}N enrichment of the samples according to Collos (1987). For kinetic and interaction experiments, relationship between uptake rates and concentrations that showed clear saturating kinetics were modeled using the original or a modified equation of the Michaelis-Menten model. When the ^{15}N-source was added at graded concentrations, uptake data were modeled using the original Michaelis-Menten relation:

$$V_N = V_{max\text{-}N} \times [N] / (K_s + [N]) \qquad (1)$$

Where V_N (in h^{-1}) is the N-uptake rate under a nutrient concentration of $[N]$ (in µmol N L^{-1}), $V_{max\text{-}N}$ is the maximal uptake rate (in h^{-1}) and K_s is the half-saturation constant (in µmol N L^{-1}). For these kinetics, the initial slope α was also calculated from the uptake rate at the concentration of 0.5 µmol N L^{-1} estimated by the model equation as recommended by Hurd and Dring (1990), and was used as an indicator of the competitive ability of the cells at low substrate concentrations.

For the interaction experiment, the exponential decrease in the uptake rate of one nutrient (N1) when increasing the concentration of the other (N2) was fitted to the reverse Michaelis-Menten relation (Varela and Harrison, 1999):

$$V_{N1} = V_{max\text{-}N2=0} \times (1 - (I_{max} \times [N2] / (K_I + [N2])) \qquad (2)$$

241 Where the N-uptake rate of the nutrient N1, V_{N1} (in h^{-1}), is function of the maximum uptake
242 rate without inhibition ($V_{max\text{-}N2=0}$, in h^{-1}), the concentration of the inhibitory nutrient *[N2]* (in
243 µmol N L^{-1}), the maximum inhibition I_{max} (values from 0 to 1) and of the inhibition constant K_I
244 (concentration of N2 at which $I = I_{max} / 2$, in µmol N L^{-1}).
245 For the diel cycle experiment, uptake rates during each light and dark period were estimated
246 from linear regressions of isotopic ratios *vs*. time.
247 Values of kinetic parameters were obtained from non-linear regressions of data sets,
248 using the Statgraphics Centurion software (Manugistics, Inc.). Statistical tests (significance and
249 comparison of regression slopes) were performed using the same software.
250

251 # 3. Results

252

253 ## 3.1. Culture medium and cellular growth

254 In terms of nutrient availability, low N-conditions were verified in the culture medium
255 used for running the experiments. The medium used for resuspension and incubation of *O.* cf.
256 *ovata* cells was characterized by an NH_4^+ concentration of 0.82 µmol N L^{-1} (SD± 0.27 µmol N
257 L^{-1}) and NO_3^- concentration of 1.00 µmol N L^{-1} (SD± 0.01 µmol N L^{-1}).
258 All cultures used for running the experiments were growing exponentially, under similar
259 growth conditions. At resuspension time, the growth rates of replicated cultures were, on
260 average, 0.39 d^{-1}, 0.45 d^{-1} and 0.51 d^{-1} for the kinetic experiment, the interaction experiment
261 and the diel cycle experiment, respectively. Quantities of particulate organic nitrogen (PN) and
262 carbon (PC) allowed for estimations of C:N (atomic) ratio. Mean C:N ratios of 12.3 (SD± 1.0)
263 and 12.5 (SD± 0.8) were estimated for the strains MCCV 054 and MCCV 055, respectively,
264 from the compilation of data sets obtained during short-term experiments (1h-incubations).
265 Extra-cellular mucilage might have interfered in the precision of these estimations. Trends

observed in C:N ratios did not allow for a detailed characterization of the coupling between N- and C-fluxes over the diel cycle.

3.2. Uptake rates during kinetic experiments

Variations of ^{15}N-enrichment over 1h-incubations showed that *O.* cf. *ovata* cells were able to use dissolved inorganic N-sources (NH_4^+ and NO_3^-) and dissolved organic nitrogen (N-urea). Similar saturating kinetic curves were observed for the two strains of *O.* cf. *ovata* tested, when NH_4^+, NO_3^- or N-urea was added as a unique N-source along a gradient of 0 – 10 µmol N L^{-1} (Figure 1). Out of the three potential N-sources tested, *O.* cf. *ovata* cells showed a clear preference pattern following the ranking: $NH_4^+ > NO_3^- >$ N-urea. No potential preconditioning effect influenced this ranking because *O.* cf. *ovata* cells were grown in K/10 medium with NH_4^+ and NO_3^- added as N-sources and an acclimation of cells to the presence of N-urea in the culture medium did not induce a clear modification of N-urea kinetics (Figure 1C). For both strains, on average along the whole gradient, NH_4^+ uptake rate was 4 to 5 times higher than NO_3^- uptake rate, when NO_3^- uptake rate was 8 to 9 times higher than N-urea uptake rate.

Relationships between uptake rates and nutrient concentrations were characterized by the Michaelis-Menten model. Similar estimations of kinetic parameters (V_{max}, K_s, α) were obtained for the two strains (Table 1). This similarity allowed to characterize abilities of *O.* cf. *ovata* cells isolated in the Bay of Villefranche-sur-mer by a maximal uptake rate (V_{max}) of 0.021 h^{-1} (SD± 0.001 h^{-1}), 0.008 h^{-1} (SD± 0.003 h^{-1}), 0.0005 h^{-1} (SD± 0.0001 h^{-1}) for NH_4^+, NO_3^- and N-urea, respectively. The associated K_s values were 0.5 µmol N L^{-1} (SD± 0.1 µmol N L^{-1}), 2.3 µmol N L^{-1} (SD± 2.1 µmol N L^{-1}) and 0.3 µmol N L^{-1} (SD± 0.1 µmol N L^{-1}) for NH_4^+, NO_3^- and N-urea, respectively. For the characterization of abilities under low nutrient concentrations, the initial slope of kinetic curves (α) was 0.011 L µmol N^{-1} h^{-1} (SD± 0.001 L µmol N^{-1} h^{-1}),

290 0.002 L µmol N^{-1} h^{-1} (SD± 0.001 L µmol N^{-1} h^{-1}) and 0.0003 L µmol N^{-1} h^{-1} (SD± 0.0001 L
291 µmol N^{-1} h^{-1}) for NH_4^+, NO_3^- and N-urea, respectively.
292
293 **3.3. Uptake rates during interaction experiments**
294 The influence of NH_4^+ on the maximal uptake rate of NO_3^- ($V_{max\text{-}NO3\text{-}}$) was analyzed
295 from estimations of $^{15}NH_4^+$ and $^{15}NO_3^-$-uptake rates after an addition of 10 µmol N L^{-1} of NO_3^-
296 and an NH_4^+ concentration varying from 0 to 10 µmol N L^{-1} (Figure 2A). In the presence of 10
297 µmol N L^{-1} of NO_3^-, the relationship between NH_4^+ uptake rate and NH_4^+ concentration
298 displayed a saturating kinetic (Figure 2A) with a high V_{max} of 0.034 h^{-1} and a K_s value (0.7 µmol
299 N L^{-1}) close to estimations done when NH_4^+ was added as the only N-source (Table 1).
300 Variations of $V_{max\text{-}NO3\text{-}}$ along the NH_4^+ gradient showed an exponential decrease that could be
301 characterized by fitting the data set to the reverse Michaelis-Menten model (2) (Figure 2A).
302 The inhibition parameters generated by the model (Table 1) showed a strong NH_4^+ inhibition
303 of NO_3^- uptake rate, with a maximum inhibition value of 67% and a K_I value of 6.2 µmol N L^{-1}.
304
305 Under reverse nutrient conditions (addition of 10 µmol N L^{-1} of NH_4^+ along a NO_3^-
306 gradient of 0-10 µmol N L^{-1}), variations of NO_3^- uptake rates were characterized by kinetic
307 parameters (V_{max} = 0.008 h^{-1}, K_s = 2.8 µmol N L^{-1}) after fitting the data set to the Michaelis-
308 Menten model (1) (Figure 2B, Table 1). Concerning variations of $V_{max\text{-}NH4+}$ with increasing
309 NO_3^- concentration, the reverse Michaelis-Menten model did not converge, however, even if
310 the NH_4^+ uptake rate obtained after addition of 10 µmol N L^{-1} of NH_4^+ and 10 µmol N L^{-1} of
311 NO_3^- appeared to be slightly low Figure 2B). Globally, NH_4^+ uptake rate was stable along the
312 NO_3^- gradient, with $V_{max\text{-}NH4+}$ = 0.026 h^{-1} (SD± 0.002 h^{-1}).
313
314 **3.4. Diel cycle experiment**

After the addition of 100 µmol N L^{-1} of ^{15}N ($^{15}NH_4^+$ or $^{15}NO_3^-$), linear decreases in nutrient concentrations were observed with time for both series of incubations (data not shown). Despite the consumption of nitrogen sources, final concentrations of NH_4^+ and NO_3^- in replicated flasks were 84 µmol N L^{-1} (SD± 9 µmol N L^{-1}) and 82 µmol N L^{-1} (SD± 4 µmol N L^{-1}), respectively, after 24h of incubation. These estimations showed the maintenance of N-replete conditions over the whole experiment duration (24h).

According to estimations of ^{15}N-enrichment of *O.* cf. *ovata* cells over the diel cycle, microalgal cells were capable of using both NH_4^+ and NO_3^- during the light and the dark periods (Figure 3). For both NH_4^+ and NO_3^-, linear increases in ^{15}N-atom (%) of *O.* cf. *ovata* cells were observed with time during each consecutive light and dark periods. During the first light period, trends were highly significant for both NH_4^+ and NO_3^- (linear regressions with $r^2 = 0.99$, $p < 0.001$, Table 2 and Figure 3). Slopes of linear regressions allowed for precise estimations of N-uptake rates and indicated that NH_4^+-uptake rate was higher (0.032 h^{-1}) than but also close to NO_3^--uptake rate (0.030 h^{-1}) during the light period. During the subsequent dark phase, values of ^{15}N-atom (%) were coherent between replicated flasks and showed an increasing trend with time for both NH_4^+ and NO_3^- (Figure 3). Slopes of linear regressions that modelled dark processes were not significant ($r^2 \geq 0.78$, $p \geq 0.06$, Table 2), however, suggesting a lack of precision in dark N-uptake rate estimations. From present results, dark uptake rates corresponded to 19% and 10% of light uptake rates for NH_4^+ and NO_3^-, respectively.

4. Discussion

Nutrient uptake capabilities of phytoplankton cells are known to vary as a function of cell size (Litchman et al., 2007), nutritional history and physiological status of the cells (Mulholland and Lomas, 2008), growth rates (Maguer et al., 2007), N substrate interactions

(Maguer et al., 2007; Jauzein et al., 2008a) and environmental factors such as irradiance and temperature (Lomas and Glibert, 1999; Kudela and Cochlan, 2000). Consequently, it is often difficult to determine taxa-specific differences in uptake capabilities and environmental control on uptake from field studies. Characterization of uptake capabilities under controlled conditions from culture studies gives the opportunity to better understand uptake regulation. Relatively few studies have determined N-uptake kinetics from cells that are nitrogen replete. In previous culture works, kinetic parameters were often characterized for cells under N-limited conditions or after several days of N-starvation (e.g. Nishikawa et al., 2009; Kwon et al., 2013). Nutrient depletion can lead to transient or surge uptake, however, when an uncoupling between nutrient uptake and growth occurs (Dortch et al., 1982; Mulholland and Lomas, 2008). In the present study, efforts were made at characterizing N-uptake of cells growing under optimal conditions. Experiments started by the resuspension of exponentially growing cells in –N medium, when physical conditions were optimized to ensure no limitation of uptake capabilities. Ammonium concentrations used to monitor uptake rates were also lower than concentrations known to potentially inhibit growth of dinoflagellate cells (Collos and Harrison, 2014; Siu et al., 1997). Thus, patterns and non-linear regressions of data sets obtained allow for the characterization and parameterization of functional responses of *O.* cf. *ov*ata cells to N-sources availability. In particular, values of parameters, such as half-saturation constants and inhibition parameters, are crucial for ecological modeling and understanding of forcing functions (Tian, 2006). In the present study, estimations were done when uptake of microalgal cells was tightly coupled with growth; values of parameters obtained can be used for the definition of mechanistic formulations that simulate the function for nutrient limitation of *O.* cf. *ov*ata growth.

Nutrient uptake by microalgal cells is an active process, whose response to extracellular nutrient concentration can generally be modelled as that of an enzyme, using Michaelis-Menten kinetics. In the Michaelis-Menten model, the maximum uptake rate (V_{max}) and half-saturation

365 constant (K_s) are often said to be biological parameters, dependent on the number of carrier
366 sites on cell membrane and specific efficiency of each transporter (Aksnes and Egge, 1991;
367 Litchman et al., 2007). Estimations of these parameters, along with the affinity coefficient α,
368 have been used to assess the relative preference for different N-substrates or competitive
369 abilities between species under various nutritive conditions (Cochlan et al., 2008; Mulholland
370 and Lomas, 2008). In the present study, kinetic curves were characterized in the range of few
371 µmol N L^{-1}, for two strains isolated during the same bloom event. They show that *O.* cf. *ovata*
372 cells are able to use dissolved inorganic N-sources (NO_3^- and NH_4^+) and dissolved organic
373 sources (N-urea) with a clear preference pattern: this pattern follows the ranking $NH_4^+ > NO_3^-$
374 > N-urea and was well defined all over the gradient tested (0.1 – 10 µmol N L^{-1}).
375 Preconditioning effects did not interfere in these trends for neither of the N-sources tested.
376 Results also show that the preferential uptake of NH_4^+ relative to NO_3^- is accentuated for *O.* cf.
377 *ovata* cells by an inhibitory effect of NH_4^+ concentration on NO_3^- uptake capabilities.
378 Conversely, no influence of NO_3^- availability on NH_4^+ uptake was observed for this species.
379 Repression of NO_3^- uptake by NH_4^+ has been well studied for many decades for several
380 phytoplankton species (Glibert et al., 2016), but never for benthic dinoflagellates. The maximal
381 inhibition estimated for *O.* cf. *ovata* cells (I_{max} = 67%) is similar to values reported for other
382 dinoflagellates (*Alexandrium minutum*, *Prorocentrum minimum*, *Gyrodinium uncatenum*)
383 (Lomas and Glibert, 1999; Maguer et al., 2007). The half-inhibition constant (K_I) estimated for
384 *O.* cf. *ovata* (6.2 µmol N L^{-1}) appears really high compared to values reported in previous
385 studies, however, in particular for N-sufficient microalgal cells (e.g., Lomas and Glibert, 1999;
386 Maguer et al., 2007); this suggests a low sensitivity of NO_3^- uptake of *O.* cf. *ovata* cells to NH_4^+
387 concentration, in particular under low NH_4^+ availability.

388 On a broader point of view, NH_4^+ is commonly found to be the preferred N-source over
389 NO_3^- and N-urea for phytoplankton uptake (Mulholland and Lomas, 2008; Glibert et al., 2016,

and references therein). The preferential use of NH_4^+ is attributed largely to the low energetic demand for its uptake and assimilation (Syrett, 1981). Exceptions have been documented, however, such as the preference of *Pseudo-nitzschia australis* for NO_3^- over NH_4^+ and N-urea reported by Cochlan et al. (2008). Most importantly, the preference for NH_4^+ over NO_3^- may strongly depend on the range of nutrient considered. As well explained and conceptualized by Glibert et al. (2016), the preference for NH_4^+/NO_3^- can be inverted under high nutrient conditions, due to either *(i)* the toxicity and growth inhibition of high NH_4^+ concentrations and/or *(ii)* the potential acceleration of NO_3^- uptake in the presence of NO_3^- that can lead to biphasic kinetics. In the present study, results suggest that such an acceleration on NO_3^- uptake occurs for *O* cf. *ovata* cells exposed to high NO_3^- concentrations. Indeed, NH_4^+ uptake rates were 4 to 5 times higher than NO_3^- uptake rates during kinetic experiments that were conducted in the range 0.1 – 10 µmol N L^{-1}. During the light period of the diel-cycle experiment, estimations of mean NO_3^- uptake rate (0.030 h^{-1}) were close to estimations of mean NH_4^+ uptake rate (0.032 h^{-1}) after addition of 100 µmol N L^{-1} of NH_4^+ or NO_3^-, however. This mean NO_3^- uptake rate obtained under high nitrate concentrations was more than 3 times higher than the V_{max} value of 0.008 h^{-1} estimated in the range 0.1 – 10 µmol N L^{-1}. Such variations in N-uptake capabilities are consistent with the existence of a two-component NO_3^- uptake system, involving a high-affinity low-capacity constitutive component and a low-affinity high capacity inducible uptake component (Glibert et al., 2016). Results obtained in the present study are consistent with the threshold of about 60 µmol N L^{-1} that was reported for the transition between biphasic kinetics of NO_3^- uptake for several phytoplankton species (Collos et al., 1992; Lomas and Glibert, 2000).

The monitoring of N-uptake rates done over the diel cycle allows for the characterization of dark N-uptake capability of *O* cf. *ovata* under N-sufficient conditions. Dark uptake of N compounds is commonly observed in marine waters (e.g. Cochlan et al., 1991; Fan and Glibert,

2005; Maguer et al., 2015). For photosynthetic cells, nutrient uptake and assimilation in darkness occurs at the expense of previously accumulated carbon that will supply dark processes with energy (ATP), reductant (NAD(P)H) and C-skeletons (Turpin, 1991). Photosynthetic carbon can be stored in excess during the light period into C-rich and N-free macromolecules, such as carbohydrates (Clark and Flynn, 2002; Granum et al., 2002) or neutral lipids (Fabrégas et al., 2002). Detailed observations of morphological and metabolic features *O*. cf. *ovata* cells revealed that their cytoplasm is often full of neutral lipid droplets, in all stages of growth under N-sufficient conditions (Honsell et al., 2013). This suggests a potential for C-storage strategies that could support dark processes. Various taxonomic groups of phytoplankton, including dinoflagellates, prymnesiophytes and diatoms, carry out uptake at night under N-sufficient conditions (e.g. Paasche et al., 1984; Clark et al., 2002; Needoba and Harrison, 2004), with reported dark:light (D/L) uptake ratios ranging from 1% to 75% for NO_3^- and from 21% to 100% for NH_4^+ (Jauzein et al., 2011, and references therein). With D/L uptake ratios of 10% and 19% measured for NO_3^- and NH_4^+ in the present study, *O*. cf. *ovata* shows low capabilities for N-uptake in darkness, at least under N-sufficient conditions. Thus, the lipid storage strategy noted by Honsell et al. (2013) has to be explored further through additional experiments to define its implications in the species competitiveness. As dark N-uptake processes have been shown to be enhanced under N-limited conditions (Paasche et al., 1984; Turpin, 1991), it could also be interesting to complete the characterization of dark N-uptake capabilities of *O*. cf. *ovata* testing N-limited conditions and/or *in situ* measurements.

According to present results, ability to take up nutrients in darkness cannot be seen as a competitive advantage for *O*. cf. *ovata*. Additional information about species competitiveness can be defined from nutrient uptake kinetic parameters (e.g. Smayda, 1997; Litchman et al., 2007). On a broad point of view, reviews of parameter values reported in both field studies and experimental works show that dinoflagellates have generally higher K_s for DIN than diatoms

(Smayda, 1997; Kudela et al., 2010). Diatoms were also characterized by higher carbon-specific V_{max} (values standardized by C units in order to diminish the effect of cell size) for NO_3^- than other taxa, including dinoflagellates (Litchman et al., 2007). Thus, a general trend of low competitive abilities for acquisition of DIN can be defined for dinoflagellates that puts emphasis on the contribution of organic matter in fueling dinoflagellate blooms in oligotrophic or mesotrophic coastal waters (e.g. Collos et al., 2004).

For the benthic compartment in particular, studies reporting uptake parameters are rare. Estimations of NO_3^- uptake kinetics were done for several species of benthic diatoms by Kwon et al. (2013) and for *O*. cf. *ovata* by Pistocchi et al. (2014). These studies report surprisingly high K_s values (ranging from 6.75 µmol N L^{-1} to 9.29 µmol N L^{-1}) compared to literature on planktonic species (Kudela et al., 2010). For *O*. cf. *ovata*, K_s value reported by Pistocchi et al. (2014) (8.4 µmol N L^{-1}) is strongly higher than values (< 4 µmol N L^{-1}) obtained in the present study for strains isolated from French coastal waters. Strong differences in N-uptake abilities can be observed between strains of the same species (Jauzein et al., 2008b). It has also to be noted that some methodological choices can partly explain the high level of K_s reported in Kwon et al. (2013) and Pistocchi et al. (2014) for NO_3^- uptake of benthic species. These studies were conducted on a large NO_3^- concentration gradient, ranging from 1 µmol N L^{-1} to 100 µmol N L^{-1}, when kinetic experiments of the present study were run on 0.1-10 µmol N L^{-1}. Collos et al. (2005) pooled data from 20 different studies dealing with phytoplankton uptake and showed a direct increase in K_s values with maximal NO_3^- concentration used in the respective studies. This correlation can be explained by an acclimation of microalgal cells to high NO_3^- concentrations coming from the existence of multiphasic uptake systems (Collos et al., 2005; Glibert et al., 2016); as explained above, such a biphasic system is suspected for *O.* cf. *ovata*. Thus, kinetic parameters estimated by Kwon et al. (2013) and Pistocchi et al. (2014) are probably representative of microalgal cell responses to high nutrient availability, but might not

provide an appropriate representation of uptake capabilities under low N-conditions, making these results hardly comparable to the present study.

Uptake kinetics are also known to potentially vary with N-history and physiological status of microalgal cells (Mulholland and Lomas, 2008). When compiling exclusively results obtained from actively growing cultures, kinetic parameter values determined for NH_4^+, NO_3^- and N-urea uptake by *O.* cf. *ovata* in the present study are in accordance with values reported for other planktonic dinoflagellates (Table 3). For NO_3^-, the compilation of these data sets also highlights higher V_{max} for diatoms compared to dinoflagellates, when no pattern can be defined for K_s (Table 3).

In the Bay of Villefranche-sur-mer (South of France), nutritive conditions can be seen as oligotrophic to mesotrophic (Selmer et al., 1993). Recent blooms of *O*. cf. *ovata* in this bay were observed when NH_4^+, NO_3^- and N-urea concentrations ranged between 0.04 – 0.27 µmol N L^{-1}, 0.20 – 2.12 µmol N L^{-1} and 0.3 – 2.25 µmol N L^{-1}, respectively (data not shown). Under such low availability in N-sources, affinity (K_s) more than velocity (V_{max}) should control species competitiveness. In the present study, values of K_s estimated for NH_4^+, NO_3^- and N-urea uptake by *O*. cf. *ovata* are in the upper part of these ranges of *in situ* concentrations. This suggests a good adaptation of the cells to field conditions but not a strong affinity strategy. To go further on the definition of specific competitive abilities, affinity for N-sources can also be compared to other taxa taking into account field studies and other culture works. Indeed, characterization of N-uptake kinetics of microalgal cells as a function of N-limitation did not always show variations of K_s with N-status or cell nutritional history (Hu et al., 2014; Maguer et al., 2007). According to the review done by Kudela et al. (2010), *O.* cf. *ovata* shows relatively high K_s (low affinity) for NO_3^-, as most of the dinoflagellates do, but a low K_s for NH_4^+ compared to both dinoflagellates and diatoms. This defines strong competitive abilities of *O.* cf. *ovata* for NH_4^+ uptake under low N-conditions, like the ones encountered during bloom seasons in the

Bay of Villefranche-sur-mer. Mixotrophic abilities of *O.* cf. *ovata* have not been fully characterized yet and are still a matter of debate (Escalera et al., 2014). Current results characterize the potential use of N-urea as a source of labile DON for *O.* cf. *ovata* cells. According to uptake capabilities and ranges of *in situ* conditions, contribution of N-urea to growth of *O.* cf. *ovata* in Villefranche-sur-mer Bay is probably low compared to DIN sources, even if this source can be rapidly regenerated in the water column (Lomas et al., 2002). Out of the three N-sources tested in the present study, the main N-source fueling blooms *O.* cf. *ovata* in the Bay of Villefranche-sur-mer is probably NH_4^+, a recycled N-source for which *O.* cf. *ovata* showed highest uptake rates and good competitive abilities.

5. Conclusions

The present study provides a detailed parameterization of N-uptake by *O.* cf. *ovata*. Kinetic and inhibition parameters can be used for the definition of mechanistic formulations in order to simulate growth limitation by nutrient availability. Ability to take up nutrients in darkness could not be defined as a competitive advantage for *O.* cf. *ovata* during exponential growth. Conversely, a strong affinity for NH_4^+ was observed for *O.* cf. *ovata* cells and may partly explain the success of this species during the summer season in the Bay of Villefranche-sur-mer (France). Further studies will be necessary to clarify the role of organic matter in growth of *O.* cf. *ovata* cells during bloom development and maintenance. It could also be interesting to better characterize links between C fluxes and other metabolic processes in *O.* cf. *ovata* cells, trying to define for example the potential role of the lipid storage strategy in terms of species competitiveness.

Acknowledgements

The authors are grateful to Sophie Marro for isolating and maintaining the algal strains. Those experiments were done with the financial assistance of the European Union under the ENPI CBC Mediterranean Sea Basin Programme, within the project M3-HABs (Project Reference Number: IIB/ 2.1/0096). The authors also wish to thank the French National Project ANR OCEAN 15 for its contribution for the financial support and the fruitful discussions with project members. Our group is part of the national French GDR PHYCOTOX (CNRS and Ifremer). The authors also have deep thoughts for Yves Collos who inspired this work.

References

Accoroni, S., Romagnoli, T., Colombo, F., Pennesi, C., Di Camillo, C.G., Marini, M., Battocchi, C., Ciminiello, P., Dell'Aversano, C., Dello Iacovo, E., Fattorusso, E., Tartaglione, L., Penna, A., Totti, C., 2011. *Ostreopsis* cf. *ovata* bloom in the northern Adriatic Sea during summer 2009: Ecology, molecular characterization and toxin profile. Mar. Pol. Bull. 62, 2512-2519.

Accoroni, S., Romagnoli, T., Pichierri, S., Totti, C., 2014. New insights on the life cycle stages of the toxic benthic dinoflagellate *Ostreopsis* cf. *ovata*. Harmful Algae 34, 7-16.

Accoroni, S., Glibert, P.M., Pichierri, S., Romagnoli, T., Marini, M., Totti, C., 2015. A conceptual model of annual *Ostreopsis* cf. *ovata* blooms in the northern Adriatic Sea based on the synergic effects of hydrodynamics, temperature, and the N:P ratio of water column nutrients. Harmful Algae 45, 14-25.

Accoroni, S., Totti, C., 2016. The toxic benthic dinoflagellates of the genus *Ostreopsis* in temperate areas: a review. Advances in Oceanography and Limnology 7(1), 1-15.

Aksnes, D.L., Egge, J.K., 1991. A theoretical model for nutrient uptake in phytoplankton. Mar. Ecol. Prog. Ser. 70, 65–72.

Aligizaki, K., Nikolaidis, G., 2006. The presence of the potentially toxic genera *Ostreopsis* and *Coolia* (Dinophyceae) in the north Aegean sea, Greece. Harmful Algae 5, 717-730.

Barone, R., 2007. Behavioural trait of *Ostreopsis ovata* (Dinophyceae) in Mediterranean rock pools: the spider's strategy. Harmful Algae News 33, 1-3.

Bendschneider, K., Robinson, R.J., 1952. A new spectrophotometric method for the determination of nitrite in sea water. J. Mar. Res. 11, 87–96.

Biré, R., Trotereau, S., Lemée R., Oregioni, D., Delpont, C., Krys, S., Guérin, T., 2015. Hunt for palytoxins in a wide variety of marine organisms harvested in 2010 on the French Mediterranean coast. Mar. Drugs 13, 5425-5446.

Brescianini, C., Grillo, C., Melchiorre, N., Bertolotto, R., Ferrari, A., Vivaldi, B., Icardi, G., Gramaccioni, L., Funari, E., Scardala, S., 2006. *Ostreopsis ovata* algal blooms affecting human health in Genova, Italy, 2005 and 2006. Eurosurveillance 11, e060907.3.

Brissard, C., Herrenknecht, C., Séchet, V., Hervé, F., Pisapia, F., Harcouet, J., Lemée, R., Chomérat, N., Hess, P., Amzil, Z., 2014. Complex toxin profile of French Mediterranean *Ostreopsis* cf. *ovata* strains, seafood accumulation and ovatoxins prepurification. Mar. Drugs 12, 2851–2876.

Burkholder, J.M., Glibert, P.M., Skelton, H.M., 2008. Mixotrophy, a major mode of nutrition for harmful algal species in eutrophic waters. Harmful Algae 8, 77-93.

Ciminiello, P., Dell'Aversano, C., Iacovo, ED., Fattorusso, E., Forino, M., Tartaglione, L., Benedettini, G., Onorari, M., Serena, F., Battocchi, C., et al., 2014. First finding of *Ostreopsis* cf. *ovata* toxins in marine aerosols. Environ. Sci. Technol. 48, 3532–3540.

Clark, D.R., Flynn, K.J., 2002. N-assimilation in the noxious flagellate Heterosigma carterae (Raphidophyceae): dependence on light, N-source, and physiological state. J. Phycol. 38, 503–512.

564 Clark, D.R., Flynn, K.J., Owens, N.J.P., 2002. The large capacity for dark nitrate assimilation
565 in diatoms may overcome nitrate limitation of growth. New Phytol. 155, 101–108.
566 Cochlan, W.P., Harrison, P.J., Denman, K.L., 1991. Diel periodicity of nitrogen uptake by
567 marine phytoplankton in nitrate-rich environments. Limnol. Oceanogr. 36, 1689-1700.
568 Cochlan, W.P., Herndon, J., Kudela, R.M., 2008. Inorganic and organic nitrogen uptake by the
569 toxigenic diatom *Pseudo-nitzschia australis* (Bacillariophyceae). Harmful Algae 8, 111-
570 118.
571 Cohu, S., Mangialajo, L., Thibaut, T., Blanfuné, A., Marro, S., Lemée, R., 2013. Proliferation
572 of the toxic dinoflagellate *Ostreopsis* cf. *ovata* in relation to depth, biotic substrate and
573 environmental factors in the North West Mediterranean Sea. Harmful Algae 24, 32-44.
574 Collos, Y. 1987. Calculations of N-15 uptake rates by phytoplankton assimilating one or several
575 nitrogen sources. Appl. Radiat. Isot. 38, 275–82.
576 Collos, Y., Siddiqi, M.Y., Wang, M.Y., Glass, A.D.M., Harrison, P.J., 1992. Nitrate uptake
577 kinetics by two marine diatoms using the radioactive tracer ^{15}N. J. Exp. Mar. Biol. Ecol.
578 163, 251-260.
579 Collos, Y., Gagne, C., Laabir, M., Vaquer, A., Cecchi, P., Souchu, P., 2004. Nitrogenous
580 nutrition of *Alexandrium catenella* (Dinophyceae) in cultures and in Thau Lagoon,
581 Southern France. J. Phycol. 40, 96-103.
582 Collos, Y., Vaquer, A., Souchu, P., 2005. Acclimation of nitrate uptake by phytoplankton to
583 high substrate levels. J. Phycol. 41, 466-478.
584 Collos, Y., Harrison, P.J., 2014. Acclimation and toxicity of high ammonium concentrations
585 to unicellular algae. Mar. Pollut. Bull. 80, 8-23.
586 Dortch, Q., Clayton, J.R., Thoresen, S.S., Bressler, S.L., Ahmed, S.I., 1982. Response of marine
587 phytoplankton to nitrogen deficiency: Decreased nitrate uptake vs enhanced ammonium
588 uptake. Mar. Biol. 70, 13-19.

589 Escalera, L., Benvenuto, G., Scalco, E., Zingone, A., Montresor, M., 2014. Ultrastructural
590 Features of the Benthic Dinoflagellate *Ostreopsis* cf. *ovata* (Dinophyceae). Protist 165,
591 260-274.
592 Fábregas, J., Maseda, A., Domínguez, A., Ferreira, M., Otero, A., 2002. Changes in the cell
593 composition of the marine microalga, *Nannochloropsis gaditana*, during a light:dark
594 cycle. Biotechnol. Lett. 24, 1699–1703.
595 Fan, C., Glibert, P.M., Burkholder, J.M., 2003. Characterization of the affinity for nitrogen,
596 uptake kinetics, and environmental relationships for *Prorocentrum minimum* in natural
597 blooms and laboratory cultures. Harmful Algae 2, 283-299.
598 Fan, C., Glibert, P.M., 2005. Effects of light on nitrogen and carbon uptake during a
599 *Prorocentrum minimum* bloom. Harmful Algae 4, 629-641.
600 Faust, M.A., Morton, S.L., Quod, J.P., 1996. Further study of marine dinoflagellates: the genus
601 *Ostreopsis* (Dinophyceae). J. Phycol. 32, 1053-1065.
602 Glibert, P.M., Wilkerson, F.P., Dugdale, R.C., Raven, J.A., Dupont, C.L., Leavitt, P.R., Parker,
603 A.E., Burkholder, J.M., Kana, T.M., 2016. Pluses and minuses of ammonium and nitrate
604 uptake and assimilation by phytoplankton and implications for productivity and
605 community composition, with emphasis on nitrogen-enriched conditions. Limnol.
606 Oceanogr. 61, 165-197.
607 Gorbi, S., Avio, G.C., Benedetti, M., Totti, C., Accoroni, S., Pichierri, S., Bacchiocchi, S.,
608 Orletti, R., Graziosi, T., Regoli, F., 2013. Effects of harmful dinoflagellate *Ostreopsis* cf.
609 *ovata* exposure on immunological, histological and oxidative responses of mussels
610 *Mytilus galloprovincialis*. Fish Shellfish Immunol. 35, 941–950.
611 Granum, E., Kirkvold, S., Myklestad, S.M., 2002. Cellular and extracellular production of
612 carbohydrates and amino acids by the marine diatom *Skeletonema costatum*: diel
613 variations and effects of N depletion. Mar. Ecol. Prog. Ser. 242, 83–94.

614 Guidi-Guilvard, L.D., Gasparini, S., Lemée, R., 2012. The negative impact of *Ostreopsis* cf.
615 *ovata* on phytal meiofauna from the coastal NW Mediterranean. Cryptogamie, Algologie
616 33(2), 121-128.
617 Guillard, R.R.L., 1973. Division rates. In: Stein, J. R. (Ed.), Handbook of phycological
618 methods. Culture methods and growth measurements. Cambridge University Press,
619 Cambridge, UK, pp. 289–311.
620 Herndon, J., Cochlan, W.P., 2007. Nitrogen utilization by the raphidophyte *Heterosigma*
621 *akashiwo*: Growth and uptake kinetics in laboratory cultures. Harmful Algae 6, 260-270.
622 Honsell, G., Bonifacio, A., De Bortoli, M., Penna, A., Battocchi, C., Ciminiello, P.,
623 Dell'Aversano, C., Fattorusso, E., Sosa, A., Yasumoto, T., Tubaro, A., 2013. New
624 insights on cytological and metabolic features of *Ostreopsis* cf. *ovata* Fukuyo
625 (Dinophyceae): a multidisciplinary approach. PLoS ONE 8 (2): e57291.
626 Hu, Z., Duan, S., Xu, N., Mulholland, M.R., 2014. Growth and nitrogen uptake kinetics in
627 cultured *Prorocentrum donghaiense*. PLoS ONE 9(4): e94030.
628 doi:10.1371/journal.pone.0094030.
629 Hurd, C.L., Dring, M. J., 1990. Phosphate uptake by intertidal algae in relation to zonation and
630 season. Mar. Biol. 107, 281–289.
631 Jauzein, C., Loureiro, S., Garcés, E., Collos, Y., 2008a. Interactions between ammonium and
632 urea uptake by five strains of *Alexandrium catenella* (Dinophyceae) in culture. Aquat.
633 Microb. Ecol. 53, 271–280.
634 Jauzein, C., Collos, Y., Garcés, E., Vila, M., Maso, M., 2008b. Short-term temporal variability
635 of ammonium and urea uptake by *Alexandrium catenella* (Dinophyta) in cultures. J.
636 Phycol. 44, 1136–1145.

637 Jauzein, C., Collos, Y., Laabir, M., Vaquer, A., 2011. Dark metabolism and carbon–nitrogen
638 uncoupling in the toxic dinoflagellate *Alexandrium catenella* (Dinophyceae). Harmful
639 Algae 11, 73-80.
640 Keller, M.D., Selvin, R.C., Claus, W., Guillard, R.R.L., 1987. Media for the culture of oceanic
641 ultraphytoplankton. J. Phycol. 23 (4), 633-638.
642 Kudela, R.M., Cochlan, W.P., 2000. Nitrogen and carbon uptake kinetics and the influence of
643 irradiance for a red tide bloom off southern California. Aquat. Microb. Ecol. 21, 31–47.
644 Kudela, R.M., Seeyave, S., Cochlan, W.P., 2010. The role of nutrients in regulation and
645 promotion of harmful algal blooms in upwelling systems. Prog. Oceanogr. 85, 122-135.
646 Kwon, H.K., Oh, S.J., Yang, H-S., 2013. Growth and uptake kinetics of nitrate and phosphate
647 by benthic microalgae for phytoremediation of eutrophic coastal sediments. Bioresource
648 Technol. 129, 387-395.
649 Li, J., Glibert, P.M., Alexander, J.A., 2011. Effects of ambient DIN:DIP ratio on the nitrogen
650 uptake of harmful dinoflagellate *Prorocentrum minimum* and *Prorocentrum donghaiense*
651 in turbidistat. Chin. J. Oceanol. Limn. 29 (4), 746-761.
652 Litchman, E., Klausmeier, C.A., Schofield, O.M., Falkowski, P.G., 2007. The role of functional
653 traits and trade-offs in structuring phytoplankton communities: scaling from cellular to
654 ecosystem level. Ecol. Lett. 10, 1170–1181.
655 Lomas, M.W., Glibert P.M., 1999. Interactions between NH4+ and NO3- uptake and
656 assimilation: comparison of diatoms and dinoflagellates at several growth temperatures.
657 Mar. Biol. 133, 541–551.
658 Lomas, M.W., Glibert, P.M., 2000. Comparisons of nitrate uptake, storage, and reduction in
659 marine diatoms and flagellates. J. Phycol. 36, 903-913.

660 Lomas, M.W., Trice, T.M., Glibert, P.M., Bronk, D.A., McCarthy, J.J., 2002. Temporal and
661 spatial dynamics of urea uptake and regeneration rates and concentrations in Chesapeake
662 Bay. Estuaries. 25 (3), 469-482.
663 Maguer, J.-F., L'Helguen, S., Madec, C., Labry, C., Le Corre, P., 2007. Nitrogen uptake and
664 assimilation kinetics in *Alexandrium minutum* (Dynophyceae): effects of N-limited
665 growth rate on nitrate and ammonium interactions. J. Phycol. 43, 295–303.
666 Maguer, J.-F., L'Helguen, S., Waeles, M., 2015. Effects of mixing-induced irradiance
667 fluctuations on nitrogen uptake in size-fractionated coastal phytoplankton communities.
668 Estuar. Coast. Shelf S. 154, 1-11.
669 Mangialajo, L., Bertolotto, R., Cattaneo-Vietti, R., Chiantore, M., Grillo, C., Lemée, R.,
670 Melchiorre, N., Moretto, P., Povero, P., Ruggieri, N., 2008. The toxic benthic
671 dinoflagellate *Ostreopsis ovata*: Quantification of proliferation along the coastline of
672 Genoa, Italy. Mar. Pollut. Bull. 56, 1209-1214.
673 Mangialajo, L., Ganzin, N., Accoroni, S., Asnaghi, V., Blanfuné, A., Cabrini, M., Cattaneo-
674 Vietti, R., Chavanon, F., Chiantore, M., Cohu, S., Costa, E., Fornasaro, D., Grossel, H.,
675 Marco-Miralles, F., Masó, M., Reñé, A., Rossi, A.M., Sala, M.M., Thibaut, T., Totti, C.,
676 Vila, M., Lemé e, R., 2011. Trends in *Ostreopsis* proliferation along the Northern
677 Mediterranean coasts. Toxicon 57 (3), 408–420.
678 Mulholland, M.R., Lomas, M.W., 2008. Nitrogen uptake and assimilation. In: Capone, D.G.,
679 Bronk, D.A., Mulholland, M.R., Carpenter, E.J. (Eds.), Nitrogen in the marine
680 environment, second ed. Elsevier Inc. Burlington, MA. pp. 303-384.
681 Needoba, J.A., Harrison, P.J., 2004. Influence of low light and a light:dark cycle on NO3
682 uptake, intracellular NO3, and nitrogen isotope fractionation by marine phytoplankton. J.
683 Phycol. 40, 505–516.

684 Nishikawa, T., Tarutani, K., Yamamoto, T., 2009. Nitrate and phosphate uptake kinetics of the
685 harmful diatom *Eucampia zodiacus* Ehrenberg, a causative organism in the bleaching of
686 aquacultured *Porphyra thalli*. Harmful Algae 8, 513-517.
687 Paasche, E., Bryceson, I., Tangen, K., 1984. Interspecific variation in dark nitrogen uptake by
688 dinoflagellates. J. Phycol. 20, 394–401.
689 Pagliara, P., Caroppo, C., 2012. Toxicity assessment of *Amphidinium carterae*, *Coolia* cfr.
690 *monotis and Ostreopsis* cfr. *ovata* (Dinophyta) isolated from the northern Ionian Sea
691 (Mediterranean Sea). Toxicon 60, 1203–1214.
692 Parsons, ML., Preskitt, LB., 2007. A survey of epiphytic dinoflagellates from the coastal waters
693 of the island of Hawai’i. Harmful Algae 6, 658-669.
694 Parsons, M.L, Aligizaki, K., Dechraoui Bottein, M.Y., Fraga, S., Morton, S.L., Penna, A.,
695 Rhodes, L., 2012. *Gambierdiscus* and *Ostreopsis*: Reassessment of the state of knowledge
696 of their taxonomy, geography, ecophysiology, and toxicology. Harmful Algae. 14, 107-
697 129.
698 Pistocchi, R., Pezzolesi, L., Guidi, F., Vanucci, S., Guerrini, F., Pinna, A., 2014. Inorganic
699 nutrients uptake and organic phosphorus utilization by *Ostreopsis* cf. *ovata*. In:
700 Proceedings of 16th ICHA conference. pp. 147-150.
701 Rausch de Traubenberg, C., Soyer-Gobillard, M.O., 1990. Bacteria associated with a
702 photosynthetic dinoflagellate in culture. Symbiosis 8, 117–133.
703 Rhodes, L., Adamson, J., Suzuki, T., Briggs, L., Garthwaite, I., 2000. Toxic marine epiphytic
704 dinoflagellates, *Ostreopsis siamensis* and *Coolia monotis* (Dinophyceae), in New
705 Zealand. New Zeal. J. Mar. Fresh. 34, 371–383.
706 Rhodes, L., 2011. World-wide occurrence of the toxic dinoflagellate genus *Ostreopsis* Schmidt.
707 Toxicon 57 (3), 400–407.

708 Rossi, R., Castellano, V., Scalco, E., Serpe, L., Zingone, A., Soprano, V., 2010. New palytoxin-
709 like molecules in Mediterranean *Ostreopsis* cf. *ovata* (dinoflagellates) and in *Palythoa*
710 *tuberculosa* detected by liquid chromatography–electrospray ionization time-of-flight
711 mass spectrometry. Toxicon 56 (8), 1381–1387.
712 Scalco, E., Brunet, C., Marino, F., Rossi, R., Soprano, V., Zingone, A., Montresor, M., 2012.
713 Growth and toxicity responses of Mediterranean *Ostreopsis* cf. *ovata* to seasonal
714 irradiance and temperature conditions. Harmful Algae 17, 25-34.
715 Selina, M.S., Morozova, T.V., Vyshkvartsev, D.I., Orlova, T.Y., 2014. Seasonal dynamics and
716 spatial distribution of epiphytic dinoflagellates in Peter the Great Bay (Sea of Japan) with
717 special emphasis on *Ostreopsis* species. Harmful Algae 32, 1-10.
718 Selmer, J.-S., Ferrier-Pages, C., Celario, C., Rassoulzadegan, F., 1993. New and regenerated
719 production in relation to the microbial loop in the NW Mediterranean Sea. Mar. Ecol.
720 Prog. Ser. 100, 71-83.
721 Siu, G.K.Y., Young, M.L.C., Chan, D.K.O., 1997. Environmental and nutritional factors which
722 regulate population dynamics and toxin production in the dinoflagellate *Alexandrium*
723 *catenella*. Hydrobiologia 352, 117–140.
724 Smayda, T.J., 1997. Harmful algal blooms: Their ecophysiology and general relevance to
725 phytoplankton blooms in the sea. Limnol. Oceanogr. 42 (5), 1137-1153.
726 Syrett, P.J., 1981. Nitrogen metabolism of microalgae. Can. Bull. Fish. Aquat. Sci. 210, 182-
727 210.
728 Taniyama, S., Arakawa, O., Terada, M., Nishio, S., Takatani, T., Mahmud, Y., Noguchi, T.,
729 2003. *Ostreopsis* sp., a possible origin of palytoxin (PTX) in parrotfish *Scarus ovifrons*.
730 Toxicon 42, 29–33.

731 Taylor, B.W., Keep, C.F., Hall, R.O., Jr., Koch, B.J., Tronstad, L.M., Flecker, A.S., Ulseth,
732 A.J., 2007. Improving the fluorometric ammonium method: matrix effects, background
733 fluorescence, and standard additions. J. N. Am. Benthol. Soc., 26(2), 167-17.
734 Tian, R.C., 2006. Toward standard parameterizations in marine biological modeling. Ecol.
735 Model. 193, 363–386.
736 Totti, C., Accoroni, S., Cerino, F., Cucchiari, E., Romagnoli, T., 2010. *Ostreopsis ovata* bloom
737 along the Conero Riviera (northern Adriatic Sea): Relationships with environmental
738 conditions and substrata. Harmful Algae 9:233-239.
739 Turpin, D.H., 1991. Effects of inorganic N availability on algal photosynthesis and carbon
740 metabolism. J. Phycol. 27, 14–20.
741 Uchida, H., Taira, Y., Yasumoto, T., 2013. Structural elucidation of palytoxin analogs produced
742 by the dinoflagellate *Ostreopsis ovata* IK2 strain by complementary use of positive and
743 negative ion liquid chromatography/ quadrupole time-of-flight mass spectrometry. Rapid
744 Commun. Mass Spectrom. 27, 1999-2008.
745 Varela, D.E., Harrison, P.J., 1999. Effect of ammonium on nitrate utilization by *Emiliania*
746 *huxleyi*, a coccolithophore from the oceanic northeastern Pacific. Mar. Ecol. Prog. Ser.
747 186, 67–74.
748 Vila, M., Garcés, E., Masó, M., 2001. Potentially toxic epiphytic dinoflagellates assemblages
749 on macroalgae in the NW Mediterranean. Aquat. Microb. Ecol. 26 (1), 51–60.
750 Vila, M., Abós-Herràndiz, R., Isern-Fontanet, J., Àlvarez, J., Berdalet, E., 2016. Establishing
751 the link between *Ostreopsis* cf. *ovata* blooms and human health impacts using ecology
752 and epidemiology. Scientia Marina 80 (S1), 107-115.

753

754 **Legend of figures**

755

Figure 1. Kinetic curves of NH_4^+, NO_3^- and N-urea uptake for *Ostreopsis* cf. *ovata*. Data points show variations of NH_4^+, NO_3^- and N-urea uptake rates as a function of each respective nutrient concentration for the French strains MCCV 054 (A) and MCCV 055 (B). Detailed representations of variations of N-urea uptake rate, with or without acclimation to N-urea as a N-source, are shown for MCCV 054 (C) and MCCV 055 (D). Respective modeled curves (straight lines for NH_4^+, dotted lines for NO_3^- and dashed lines for N-urea) correspond to Michaelis-Menten model and values of parameters (V_{max}, K_s, α), as well as associated r^2, are listed in Table 1.

Figure 2. Variations in NH_4^+ and NO_3^- uptake rates for the strain MCCV 054 of *Ostreopsis* cf. *ovata* after an addition of 10 µmol N L^{-1} of NO_3^- and along a graded NH_4^+ concentration of 0 to 10 µmol N L^{-1} (A), or after an addition of 10 µmol N L^{-1} of NH_4^+ and along graded NO_3^- concentration of 0 to 10 µmol N L^{-1}. The modeled curves of NH_4^+ and NO_3^- uptake data correspond to solid and dotted lines, respectively. Values of parameters used for modelling these data sets are listed in Table 1 with associated r^2 values.

Figure 3. Variations in ^{15}N isotopic ratios of *Ostreopsis* cf. *ovata* cells over 24h, after addition of 100 µmol N L^{-1} of $^{15}NH_4^+$ or $^{15}NO_3^-$. The dark period is indicated by the horizontal solid line. Vertical lines indicate standard deviations from three replicate cultures. Linear regressions of data sets are represented by solid lines and dashed lines for incubations with $^{15}NH_4^+$ and $^{15}NO_3^-$, respectively. For the first light period, equations of linear regressions are $Y = 0.0318\ X - 0.3111$ ($r^2 = 0.99$) for $^{15}NH_4^+$ incubations and $Y = 0.0300\ X - 0.3415$ ($r^2 = 0.99$) for $^{15}NO_3^-$ incubations. For the dark period, equations of linear regressions are $Y = 0.0059\ X + 0.2558$ ($r^2 = 0.99$) for $^{15}NH_4^+$ incubations and $Y = 0.0029\ X + 0.2421$ ($r^2 = 0.78$) for $^{15}NO_3^-$ incubations.

780 **Table 1. Values of kinetic parameters (V_{max} in h^{-1}, K_s in µmol N L^{-1}, α in L µmol N^{-1} h^{-1}) and inhibition parameters ($V_{max\text{-}N=0}$ in h^{-1}, K_I in**
781 **µmol N L^{-1}, I_{max}) obtained for *Ostreopsis* cf. *ovata* under various culture conditions.** Uptake abilities were characterized for three potential N-
782 sources (NH_4^+, NO_3^- and N-urea), added under graded nutrient concentrations (listed in µmol N L^{-1}), as a unique N-source or in combination with
783 another one. Non-linear regressions were based on the Michaelis-Menten model or the reverse Michaelis-Menten relation.
784

Experiment (Strain)	^{15}N-addition		Kinetic parameters			r^2
	N-source	Concentration	V_{max}	K_s	α	
Kinetics (MCCV 054)	NH_4^+	0.1 - 10	0.020	0.40	0.0114	0.92
	NO_3^-	0.1 - 10	0.006	0.80	0.0023	0.94
	N-urea	0.1 - 10	0.0005	0.28	0.0003	0.82
Acclimation to N-urea	N-urea	0.1 - 10	0.0005	0.11	0.0004	0.93
Kinetics (MCCV 055)	NH_4^+	0.1 - 10	0.021	0.58	0.0098	0.89
	NO_3^-	0.1 - 10	0.010	3.73	0.0011	0.96
	N-urea	0.1 - 10	0.0004	0.38	0.0002	0.96
Interaction NH_4^+/NO_3^- (MCCV 054)						
NH_4^+ gradient, 10 µM NO_3^-	NH_4^+	0.1 - 10	0.034	0.72	0.0139	0.95
NO_3^- gradient, 10 µM NH_4^+	NO_3^-	0.1 - 10	0.008	2.77	0.0012	0.99

	Inhibition parameters		
	$V_{max\text{-}N=0}$	K_I	I_{max}

NH_4^+ gradient, 10 μM NO_3^-	NO_3^-	10	0.013	6.24	0.67	0.91	

785

786

787

788

789 **Table 2. Estimations of ^{15}N-uptake rates (in h^{-1}) of *Ostreopsis* cf. *ovata* cells in cultures under both light and dark phases of the diel cycle.**

790 Uptake abilities were characterized for NH_4^+ and NO_3^- under N-sufficient conditions.

791

Experiment (Strain)	^{15}N-addition		Mean uptake rate	r^2 (p value)
	N-source	Concentration		
Diel cycle (MCCV 054)				
First light period	NH_4^+	100	0.032	0.99 ($p < 0.001$)
	NO_3^-	100	0.030	0.99 ($p < 0.001$)
Dark period	NH_4^+	100	0.006	0.99 ($p = 0.06$)
	NO_3^-	100	0.003	0.78 ($p = 0.12$)

792

793 **Table 3. Values of kinetic parameters (maximal uptake rate V_{max} in h^{-1} and half-saturation constant K_s in µmol N L^{-1}) reported for**
794 **phytoplankton species from culture experiments with N-sufficient cells.** Ranges of nutrient concentration used for kinetics are indicated in µ
795 mol N L^{-1}. Most of the references listed reported results obtained for actively growing N-replete cells. Some experiments were conducted from
796 recently N-depleted cultures at the end of the growth phase and are indicated with a footnote.

797

Species	Substrate	NH_4^+		NO_3^-		N-urea		Reference
	concentration	V_{max}	K_s	V_{max}	K_s	V_{max}	K_s	
Diatoms								
Chaetoceros sp.	0.01 - 40			0.110	3.10			Lomas and Glibert (2000)
Pseudo-Nitzschia australis	0.1 - 40	0.071	5.37	0.105	2.82	0.0300		Cochlan et al. (2008)[ab]
Skeletonema costatum	0.01 - 40			0.100	0.40			Lomas and Glibert (2000)
Thalassiosira weissflogii	0.01 - 40			0.170	2.80			Lomas and Glibert (2000)
Dinoflagellates								
Alexandrium catenella	0.1 - 10	0.002 - 0.026	0.1 - 6.2			0.0004 - 0.001	0.6 - 2.3	Jauzein et al. (2008b)[c]
Alexandirum minutum	0.1 - 30		0.33		0.28			Maguer et al. (2007)[d]
Ostreopsis cf. *ovata*	0.01 - 10	0.021	0.49	0.008	2.27	0.0005	0.33	Present study
Prorocentrum minimum	0.01 - 40			0.050	5.00			Lomas and Glibert (2000)
	0.4 - 30		2.48		5.18		1.82	Fan et al. (2003)
	0.2 - 20	0.046	1.25			0.0004	0.05	Li et al. (2011)
Prorocentrum donghaiense	0.1 - 50	0.075	7.10			0.0400	0.12	Hu et al. (2014)
Haptophyte								

Pavelova lutheri	0.01 - 40			0.120	22.70			Lomas and Glibert (2000)
Chlorophyte								
Dunaliella tertiolecta	0.01 - 40			0.030	11.10			Lomas and Glibert (2000)
Raphydophyte								
Heterosigma akashiwo	0.1- 12	0.028	1.44	0.018	1.47	0.0029	0.42	Herndon and Cochlan (2007)[b]

798

799

800 **Footnotes**

801 [a] Non-saturating kinetics were observed for N-urea uptake; the V_{max} value indicated for N-urea uptake of *P. asutralis* in this table corresponds to

802 the uptake rate estimated at 36 µmol N L^{-1}.

803 [b] Experiments were conducted on recently N-depleted cultures, in late growth phase.

804 [c] Reported values correspond to incubations done just after and 3h after resuspension of N-replete cells in -N medium.

805 [d] Reported values correspond to results obtained for the higest growth rate, when µ/µmax = 0.42.

A

B

N-uptake rate (h^{-1})

0.025
0.020
0.015
0.010
0.005
0.000

0 2 4 6 8 10

NH4+
NO3-
N-urea

C

D

N-urea uptake rate (× 10^{-4} h^{-1})

6
5
4
3
2
1
0

No acclimation
With acclimation

Concentration (µmol N L^{-1})

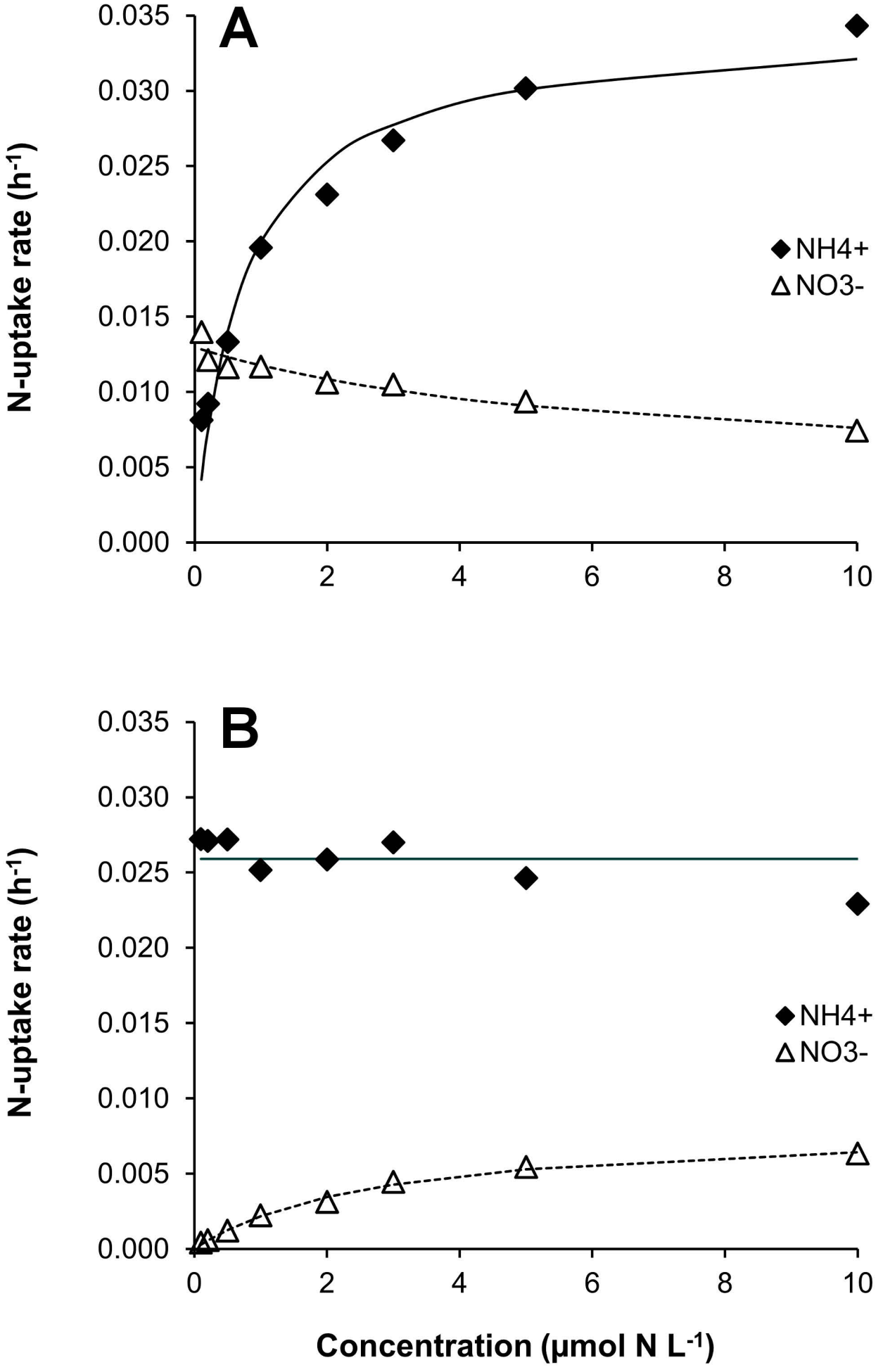
A
B
N-uptake rate (h-1)
0.035
0.030
0.025
0.020
0.015
0.010
0.005
0.000
0
2
4
6
8
10
NH4+
NO3-
Concentration (µmol N L-1)

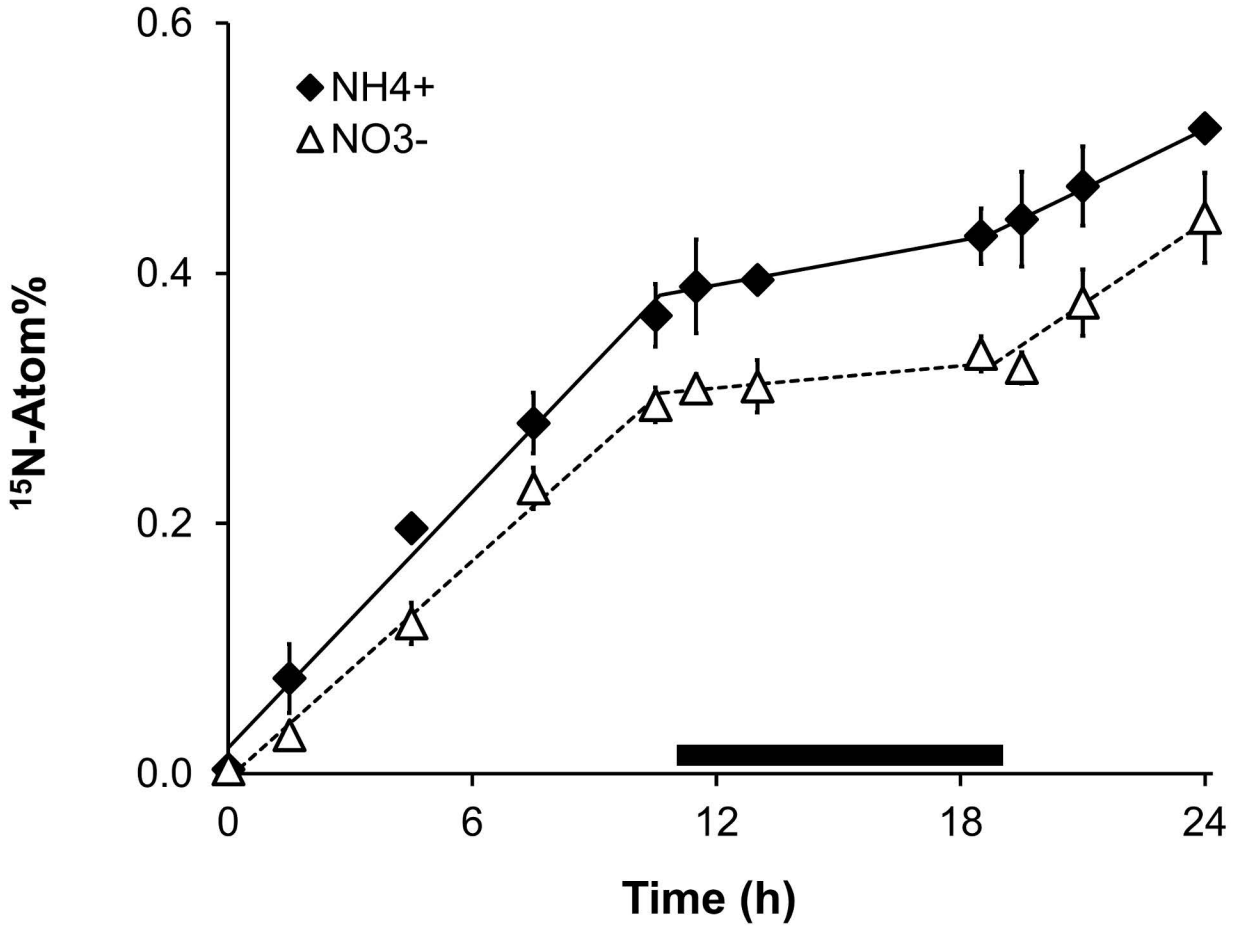
0.6
0.4
0.2
0.0
NH4+
NO3-
15N-Atom%
0
6
12
18
24
Time (h)